

# Anisotropy-driven transition from collisionless to collisional regime in the dipolar modes of a trapped gaseous mixture

P. Capuzzi <sup>\*</sup>, P. Vignolo, and M.P. Tosi

*NEST-INFM and Scuola Normale Superiore, Piazza dei Cavalieri 7, I-56126 Pisa,  
Italy*

---

## Abstract

We evaluate the dipolar oscillations of a harmonically trapped fermion gas containing thermal bosonic impurities as a function of the anisotropy of the trap, from the numerical solution of the Vlasov-Landau equations for the one-body phase-space distribution functions. Starting from a situation in which the two components of the gaseous mixture perform almost independent oscillations inside a spherical trap, we demonstrate that different collision behaviors arise for oscillations in different directions as the trap is deformed into an elongated cigar-like shape. An increase in the anisotropy of the confinement thus suffices to drive a transition of dipolar modes from a collisionless to a collisional regime.

*Key words:* Fermi gas, collisional properties, extended Kohn theorem

*PACS:* 03.75.Ss, 05.30.Fk, 02.70.Ns

---

---

<sup>\*</sup> Corresponding author, e-mail: capuzzi@sns.it

## 1 Introduction

Many aspects of the physics of ultracold quantum gases and their quantum phase transitions can usefully be explored by measuring the frequencies and the damping rates of monopolar "breathing" modes and of quadrupolar modes at various temperatures (see Ref. [1] and references therein). These measurements, which have been performed with rather high accuracy on both bosonic and fermionic systems, have been important to the understanding of Bose-Einstein condensation and of degenerate and superfluid fermion gases in confined geometries, and have become a testing ground for many-body theories.

In contrast, the dipolar "sloshing" modes in a monatomic gas under harmonic confinement contain no deep information on its microscopic behavior. These modes obey a theorem stemming from the work of Kohn [5] on a fluid of charged particles with arbitrary momentum-conserving interactions in a magnetic field, which was generalized by later workers [6] by adding an external scalar harmonic potential extending throughout all space. The theorem states that in a system of interacting particles confined by an external harmonic potential  $V_h(\mathbf{r}) = \mathbf{r} \cdot \mathbf{K} \cdot \mathbf{r}/2$  the dynamics of the center of mass is completely decoupled from that of the internal degrees of freedom. This implies sharp resonances at the bare trap frequencies for a uniform exciting field, which can only rigidly drive the density distribution of the system. The so-called extended Kohn theorem (EKT) has had important consequences in the development of time-dependent density functional theory for the dynamics of electrons in confined geometries such as quantum wells and quantum dots [7].

Turning, however, to a gaseous mixture, it is evident that its dipolar modes provide a direct signature of its collisionality [8,9]. In a regime of low collision rates the components of the mixture are independently oscillating, whereas they oscillate together when their collisionality is sufficiently high. This dynamical transition from a collisionless to a collisional (hydrodynamic) behavior has been followed both experimentally and numerically in two-component fermion mixtures [8,9]. The role played in this context by mobile impurities inside a fermion gas under spherical confinement has also been studied by numerical means [10]. Interatomic collisions also play an important role in the development and understanding of techniques for the cooling of gases in essentially harmonic confinements down to ultralow temperatures [2,3,4].

In the present work we examine the role of the anisotropy of the harmonic confinement in this dynamical transition for a fermion-boson mixture simulating a gas of fermionic  $^{40}\text{K}$  atoms which contains a small concentration of thermal  $^{87}\text{Rb}$  atoms. We numerically solve the Vlasov-Landau equations for the evolution of the phase-space distribution functions within a particle-in-cell approach (see Refs. [10,11] for the technical details). In particular, our results

demonstrate that in a cigar-shaped harmonic confinement, rigid oscillations of the centre of mass of the whole mixture in the "soft" axial direction can coexist with independent oscillations of the two components in a "hard" radial direction. This result can be considered as a further extension of the EKT.

The paper is organized as follows. In Sec. 2 we describe the mixture under study, while in Secs. 3 and 4 we analyze its dynamics under time-dependent drives. Finally, Sec. 5 offers some concluding remarks.

## 2 The physical system

The system is a mixture of spin-polarized  $^{40}\text{K}$  atoms and  $^{87}\text{Rb}$  atoms inside a magnetic trap and the interspecies interaction is modeled by a strongly repulsive contact potential characterized by an  $s$ -wave scattering length  $a = 10^4$  Bohr radii. The mixture is at low temperature and the number of  $^{87}\text{Rb}$  bosons is kept low in order to avoid the formation of a condensate, which may in turn reduce the collisionality of the system [12]. Moreover, this allows us to neglect the boson-boson interactions.

Due to the difference in masses and in internal states, fermions and bosons experience different confining potentials. These are given by

$$V_{F,B}(\mathbf{r}) = \frac{1}{2} m_{F,B} \omega_{F,B}^2 (r^2 + \lambda^2 z^2), \quad (1)$$

where we have assumed the same anisotropy parameter  $\lambda$  for the two species. In Eq. (1)  $m_{F,B}$  are the atomic masses of fermions and bosons and  $\omega_{F,B}$  are their trap frequency along the radial direction. The effects of the anisotropy will be examined by varying  $\lambda$  from 1 to 0.01 while keeping fixed the average  $\bar{\omega}_{F,B} = \omega_{F,B} \lambda^{1/3}$  of the trap frequencies. This value will be taken as the geometric average of the frequencies in the experiments carried out at LENS on the same mixture [13]. In this way we intend to explore the dependence of the dynamics solely on the anisotropy of the traps without changing other properties of the gas such as the mean densities and the chemical potentials. For definiteness we also set the temperature of the sample at  $T = 0.2T_F$  with  $T_F = \hbar \bar{\omega}_F (6N_F)^{1/3} / k_B$  being the Fermi temperature and  $N_F$  the number of fermions.

## 3 Collisionality near equilibrium

The number of collisions per unit time (*i.e.* the collision rate) in the mixture at equilibrium is both classically and quantum-mechanically independent of  $\lambda$

for fixed  $\bar{\omega}_{F,B}$ . However, a slight mismatch of the trap centers can lead to a strong decrease in the collisionality, which can be understood to be the result of the decrease in the overlap of the two density profiles. In the classical limit, the collisionality in a mixture of  $N_F$  fermions and  $N_B$  bosons reads

$$\Gamma_{\text{cl}} = \beta N_B N_F \frac{\sigma}{\pi^2} \frac{K_r^{3/2}}{m_r^{1/2}} \exp \left[ -\beta \frac{K_r}{2 \lambda^{2/3}} (x_0^2 + z_0^2 \lambda^2) \right] \quad (2)$$

when the trap centers have been offset by  $(x_0, z_0)$ . Here  $\beta = 1/k_B T$ ,  $\sigma = 4\pi a^2$  is the total scattering cross section,  $m_r$  the reduced boson-fermion mass,  $K_r = K_F K_B / (K_F + K_B)$  the effective oscillator strength, and  $K_{F,B} = m_{F,B} \bar{\omega}_{F,B}^2$  the average oscillator strength of each species. Taking  $x_0$  and  $z_0$  to be of comparable magnitudes, the collisionality as a function of the anisotropy thus displays two different trends depending on the direction of the offset.

In the numerical simulations we first shift rigidly the fermionic cloud in either the radial or the axial direction by  $a_{ho} = (\hbar/m_F \omega_F)^{1/2}$ , which is usually much smaller than the radius of the two clouds. Then the fermion cloud starts oscillating around its equilibrium position and collisions among bosons and fermions can occur. During the evolution the relative position of the centers of the two clouds changes continuously and Eq. (2) gives only an indication of the dependence of the time-averaged collisionality on  $\lambda$ . From the simulation data we have calculated the average number of collisions per unit time during a fixed time interval, that we choose to be  $\bar{t} = 10\pi/\bar{\omega}_F$ . The result is shown in Fig. 1, where we plot the average quantum collision rates  $\Gamma_q^z$  and  $\Gamma_q^r$ , corresponding to dipolar oscillations of the fermions in the two directions, as functions of the trap anisotropy  $\lambda$ . The filled symbols refer to the collision rates in units of the constant frequency scale  $\bar{\omega}_F$ .

The data in Fig. 1 show that for the system parameters that we are considering the variation with  $\lambda$  of the two collision rates  $\Gamma_q^i$  in these absolute units becomes appreciable only at low  $\lambda$ . However, referring to the empty symbols in Fig. 1 which report  $\Gamma_q^z$  and  $\Gamma_q^r$  in units of the fermionic axial and radial frequencies  $\omega_z = \lambda^{2/3} \bar{\omega}_F$  and  $\omega_r = \lambda^{-1/3} \bar{\omega}_F$ , it is seen that the numbers of collisions made on average during an oscillation period in the axial or in the radial direction are becoming very different. This suggests that, since  $\Gamma_q^r/\omega_r \ll 1$  while  $\Gamma_q^z/\omega_z$  is strongly increasing, the mixture may have a collisionless behavior along the radius  $r$  and a hydrodynamic behavior along the  $z$  axis.

The return of the system to a new equilibrium state (including instantaneous mean-field effects) can be directly investigated in the Vlasov-Landau frame by following the collision rate as a function of time. As the evolution proceeds the average number of collisions approaches that corresponding to the new equilibrium. We display in Fig. 2 the time dependence of the radial collision rate for different values of  $\lambda$ . For low-to-intermediate anisotropy the collision rate diminishes relatively rapidly towards the final equilibrium state, as can be

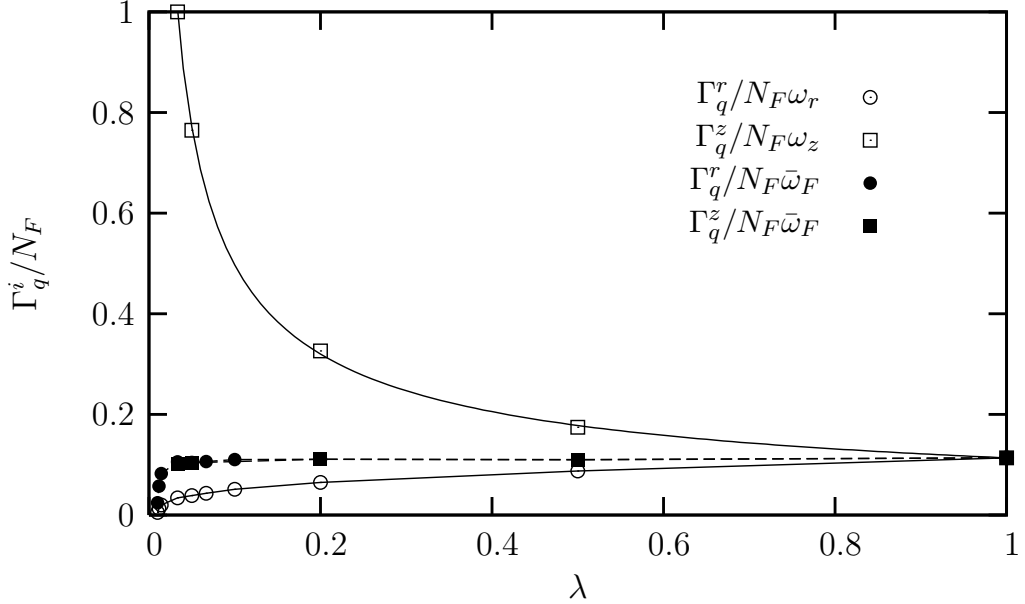


Fig. 1. Total collision rates  $\Gamma_q^i$  per fermion in the radial ( $i = r$ ) and axial ( $i = z$ ) directions, as functions of the anisotropy parameter  $\lambda$ . Filled symbols show the collision rates in units of  $\bar{\omega}_F$  and empty symbols report  $\Gamma_q^i / (N_F \omega_i)$ . The squares refer to oscillations along the radial direction and the circles to oscillations along the axis of the trap. The lines are guides to the eyes.

expected from the temperature dependence of  $\Gamma_{\text{cl}}$  in Eq. (2) since the system performs a number-conserving evolution. At higher anisotropies the evolution is much slower, *i.e.* the effective friction caused by collisions takes more time to restore equilibrium. Damping processes are evidently being quenched at high anisotropy.

#### 4 Collisionless *vs* collisional behaviour

Let us summarize some general features of the dynamical behavior of the mixture that are associated with an initial displacement of the fermion cloud, before turning to discuss the role of trap anisotropy. In the absence of interactions the fermions oscillate without damping at their bare trap frequency while the bosonic impurities remain at rest. On switching on the interactions the fermionic components sets the bosons into motion and beats between oscillations at the bosonic and the fermionic trap frequencies appear [11]. If the collision rate is much lower than the trap frequencies, the damping rate is small and the two clouds oscillate for many periods. On increasing the collisionality up to a regime where the collision rate is of the same order as the trap frequencies, the oscillation frequencies are not well defined and the center-of-mass motions of the two clouds become strongly damped. Finally,

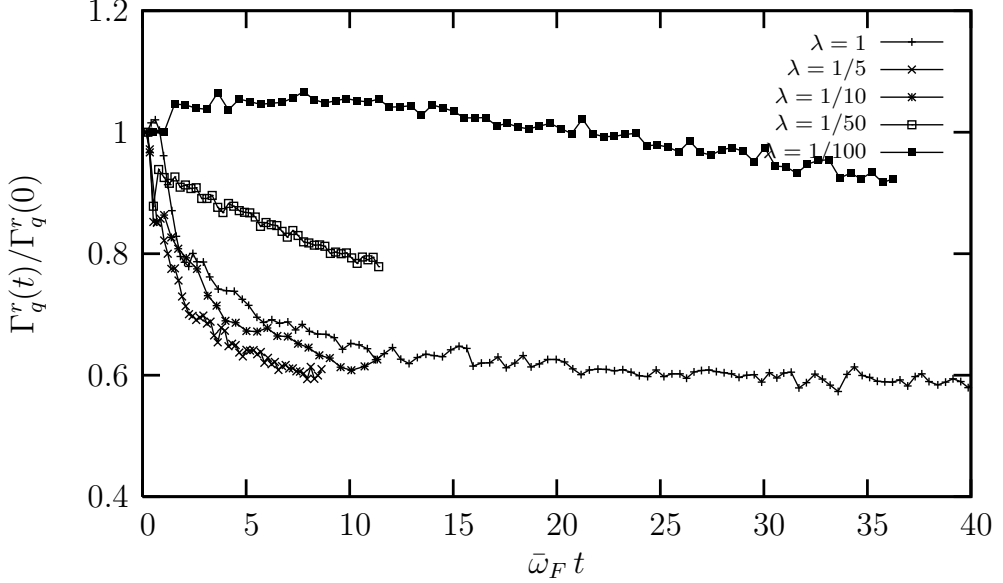


Fig. 2. Total collision rate  $\Gamma_q^r(t)/\Gamma_q^r(0)$  as a function of time for several values of the anisotropy  $\lambda$  and in the case of an initial radial displacement.

at very large collisionality the two clouds become glued together and oscillate at the same frequency without noticeable damping. Thus a clear signature of the onset of a collisional regime is the locking of the oscillations of the two components and the vanishing of their damping rates.

We turn now to examining the role played by trap anisotropy in this scenario. We plot in Fig. 3(a) the oscillation frequencies of the fermions in the radial and axial direction as functions of the anisotropy parameter  $\lambda$  which drives the collision rates referred to the trap frequencies (see Fig. 1). The data in Fig. 3 have been obtained by fitting the oscillatory motions of the fermions with functions of the form  $\cos(\Omega t + \phi) \exp(-\gamma t)$ . The oscillation frequency  $\Omega_r$  in the radial direction approaches the radial trap frequency  $\omega_r$  for low  $\lambda$  and decreases below this value with increasing  $\lambda$ . On the contrary, the oscillation frequency  $\Omega_z$  in the axial direction takes its maximum value at  $\lambda = 1$  and decreases with decreasing  $\lambda$ . These two opposite trends can be understood if we plot the oscillation frequencies as functions of the collision rates scaled by the trap frequencies. In such a plot (see Fig. 3(b)) both oscillation frequencies lie on a single monotonically decreasing curve. The plot suggests that the leftmost data correspond to collisionless radial oscillations while the rightmost data reflect an approach to the collisional regime where the axial oscillation frequencies are close to the hydrodynamic value.

To support the idea that the mixture at large trap anisotropies is in different regimes in the radial and in the axial direction, we report in Fig. 4 the damping rates  $\gamma_r$  and  $\gamma_z$  for the oscillatory motions as functions of the corresponding collision rates. In the radial direction (circles in Fig. 4) the damping rate

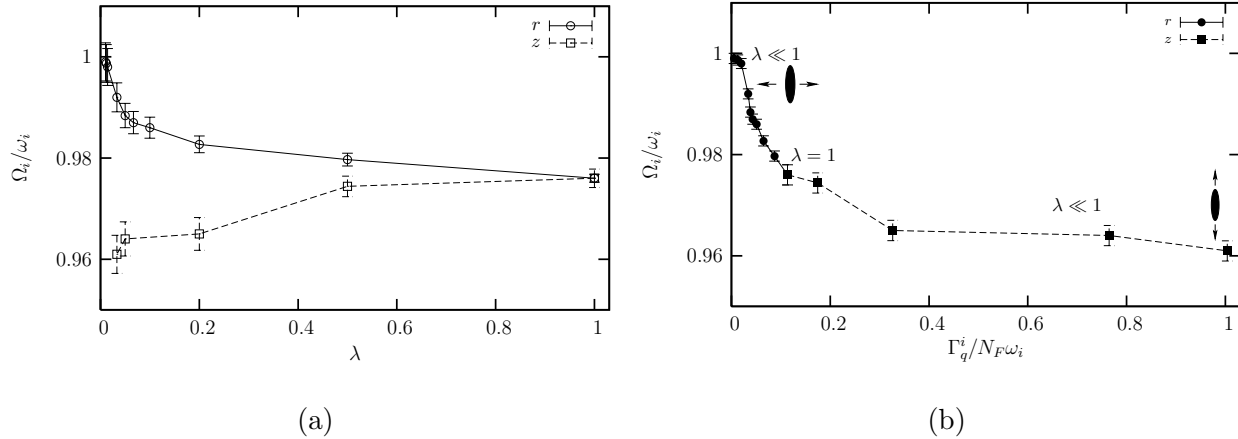


Fig. 3. Radial and axial oscillation frequencies (in units of  $\omega_r$  and  $\omega_z$ , respectively) as functions of (a) the anisotropy parameter  $\lambda$ , and (b) the collision rate  $\Gamma_q^i/N_F$  per fermion (in units of  $\omega_r$  for radial oscillations and of  $\omega_z$  for axial oscillations).

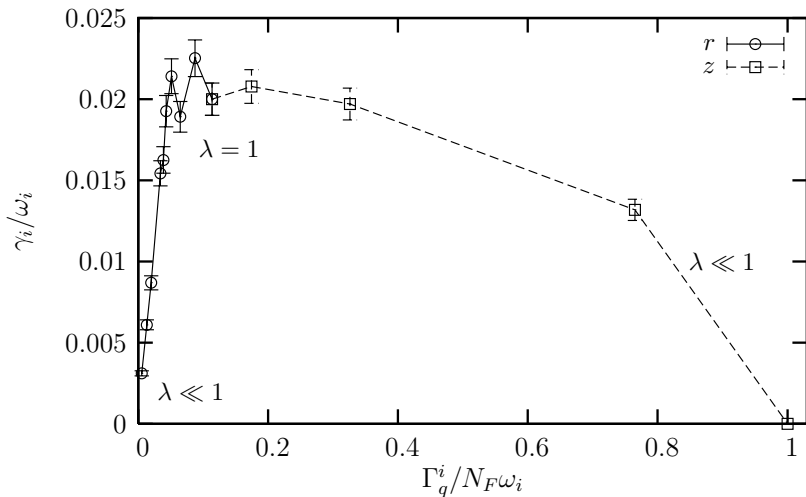


Fig. 4. Radial (circles) and axial (squares) damping rates  $\gamma_i$  (in units of  $\omega_r$  and  $\omega_z$ , respectively) as functions of the collision rates  $\Gamma_q^r/(N_F\omega_r)$  and  $\Gamma_q^z/(N_F\omega_z)$ .

increases as a function of the scaled collision rate  $\Gamma_q^r/\omega_r$  and seems to reach a maximum: this is a signature that the gas is moving from the collisionless to the intermediate collisional regime with decreasing anisotropy. On the contrary, in the axial direction (squares in Fig. 4) the damping rate decreases as a function of  $\Gamma_q^z/\omega_z$  and this is a typical behavior of an intermediate-to-collisional transition.

## 5 Conclusions

We have studied the dipolar modes of a harmonically confined fermion-boson mixture as functions of the trap anisotropy and found that, although the collisionality is independent of the anisotropy, a collisionless behavior in the radial direction and a hydrodynamic behavior in the axial direction can be simultaneously established for large anisotropies. This conclusion is based on the analysis of the dipolar oscillations of a fermion gas at ultralow temperature and containing a limited concentration of thermal bosons.

The analysis that we have presented has only regarded the dipolar oscillations of the gas. Of course, other oscillatory modes and the dynamics of a ballistic expansion would provide further insight on the physical behavior of the gas. The results of these further studies will be presented elsewhere.

## Acknowledgements

This work has been partially supported by an Advanced Research Initiative of Scuola Normale Superiore di Pisa and by the Istituto Nazionale di Fisica della Materia within the Advanced Research Project "Photonmatter" and the Initiative "Calcolo Parallelo".

## References

- [1] Minguzzi, A., Succi, S., Toschi, F. *et al.*, 2004, *Phys. Rep.*, **395**, 223.
- [2] Petrich, W., Anderson, M.H., Hensher, J.R., and Cornell, E.A., 1995, *Phys. Rev. Lett.*, **74**, 3352.
- [3] Strecker, K.E., Partridge, G.B., and Hulet, R.G., 2003 *Phys. Rev. Lett.*, **91**, 080406.
- [4] Hadzibabic, Z., Gupta, S., Stan, C.A., *et al.*, 2003, *Phys. Rev. Lett.*, **91**, 160401.
- [5] Kohn, W., 1961, *Phys. Rev.*, **123**, 1242.
- [6] Brey, L., Johnson, N.F., and Halperin, B.I. 1989, *Phys. Rev. B*, **40**, 10647; Brey, L., Dempsey, J., Johnson, N.F., and Halperin, B.I., 1990, *Phys. Rev. B*, **42**, 1240; Yip, S.K., 1991, *Phys. Rev. B*, **43**, 1707.
- [7] Dobson, J.F., 1994, *Phys. Rev. Lett.*, **73**, 2244; Vignale, G., 1995, *Phys. Rev. Lett.*, **74**, 3233.

- [8] Gensemer, S.D., and Jin, D.S., 2001, *Phys. Rev. Lett.*, **87**, 173201; DeMarco, B., and Jin, D.S., 2002, *Phys. Rev. Lett.*, **88**, 040405.
- [9] Toschi, F., Vignolo, P., Succi, S., and Tosi, M.P., 2003, *Phys. Rev. A*, **67**, 041605.
- [10] Capuzzi, P., Vignolo, P., Toschi, F., *et. al.*, submitted.
- [11] Toschi, F., Capuzzi, P., Succi, S., *et al.*, 2004, *J. Phys. B*, **37**, S91.
- [12] Timmermans, E. and Côté, R., 1998, *Phys. Rev. Lett.*, **80**, 3419.
- [13] Ferlaino, F., Brecha, R.J., Hannaford, P., *et al.*, 2003, *J. Opt. B*, **5**, S3.